CAMBRIDGE
UNIVERSITY PRESS

RESEARCH ARTICLE

Phase oscillator optimization eliminates jittering during transition gaits in multimodal locomotion assisted by a portable hip exoskeleton

Wei Yang[1,2] , Zehao Yan[1,2], Linfan Yu[1,2], Linghui Xu[1,2], Xiaoguang Liu[3] and Canjun Yang[2]

[1]Ningbo Innovation Center, Zhejiang University, Ningbo, China, [2]College of Mechanical Engineering, Zhejiang University, Hangzhou, China, and [3]Spinal Cord Injury Rehabilitation Department, Ningbo Rehabilitation Hospital, Ningbo, China
Corresponding author: Xiaoguang Liu; Email: melecture@126.com

Abstract

To be successfully used in daily life situations, exoskeletons should be effective across multimodal scenarios, including walking on various terrains, and transitions between locomotion modes such as walking-to-stop. Correct continuous gait phase estimation is essential for high-level walking assistance control. Despite the impressive advances in gait phase estimation for a variety of locomotion modes, transition gait phase estimation is rarely researched, leading to the jittering of exoskeletons during walking-to-stop transitions. We propose an optimized phase oscillator (PO-opt) that estimates the gait phase correctly during transition gaits in multimodal locomotion, which is beneficial to eliminating the jittering. In the phase plane, a lateral axis extreme difference (LAED) is adopted to classify transition gaits. The threshold of LAED for transition gaits in multimodal locomotion was preliminarily determined by simulation, which was then applied and validated in experiments. Simulation results indicated that a threshold of 15.0 was suitable for transition gaits classification during treadmill walking, free walking, and ramp ascent/descent, while results of the experiment showed that a threshold between 6.5 and 10.5 was applicable for treadmill walking, free walking, and stair ascent/descent. In particular, the jittering elimination rates for 3, 4, and 5 km/h treadmill walking were improved from 29%, 21%, and 4% (PO model) to 100%, respectively, when the threshold of LAED was set at 15.0 in PO-opt model. The results indicated a significant increase in the rate of jittering elimination when the PO-opt model was applied. The model holds great promise in real-world applications for prostheses and other types of exoskeletons.

1. Introduction

Lower limb exoskeletons are promising solutions to enhance human locomotion performance and assist walking rehabilitation [1–3]. Recent advances in the newest-generation robotic exoskeletons [4–7] have demonstrated great potential to reduce metabolic expenditure [4, 6, 8–10] and muscle activity [11, 12] and concerned user preference within the control loop [13, 14] as well. However, some specific issues still need to solve for better daily life human–exoskeleton interaction [15], for example, the gait phase estimation of walking-to-stop transition gaits during multimodal locomotion scenarios.

Continuous gait phase, a variable representing the gait period, is defined as a linearly increasing value from 0 to 100% [16]. Compared to discrete gait events, the continuous gait phase accords with actual human locomotion closely. Thus, continuous gait phase estimation is widely researched, which is essential for assistive torque profile generation. Adaptive oscillator (AO), which is widely applied for exoskeleton control [17–19], is a typical algorithm capable of predicting periodic and quasi-periodic motion through the pattern learned from preceding cycles. With a pool of AOs, the signal frequency can be converged [20], and thus, the continuous gait phase is obtained. The time-based estimation (TBE) estimates the gait period by force-sensitive resistors under the heel. The current phase inside each gait

period is obtained as the ratio between the time elapsed from the start of the current period and the expected duration of the whole period [21]. Kim et al. [4] and Zhang et al. [22] adopted the TBE method for untethered and tethered exoskeleton control, respectively. Inseung et al. [16, 23] proposed a neural network-based (NN) gait phase estimation method for real-time multimodal locomotion applications. Besides, Sugar et al. [24] designed a simple phase oscillator (PO) for continuous gait phase estimation. The gait phase is mapped to the angle between angle vector and angular velocity vector on the phase plane [25, 26]. Both AO and TBE methods are limited to periodic and quasi-periodic gait patterns. In other words, when applied to transition gaits, for example, walking to standing, the estimated gait phase error may raise significantly. NN method is robust to multimodal locomotion and transition gaits once the model is trained concerning these gaits. However, this machine learning method is training data-dependent and computationally intensive. For PO method, although the estimated gait phase linearity is affected, it is adaptive to nonperiodic gait patterns and low computing power cost. Optimized PO (PO-opt) method is beneficial to improving the robustness to multimodal locomotion and transition gaits. We propose a PO optimization approach, which "shifts," "scales," and "slices" the angle–angular velocity portrait on the phase plane, to reduce gait phase estimation errors and classify the correct state for walking-to-stop transition gaits during multimodal locomotion assisted by a portable hip exoskeleton.

The overall aim of this work was to verify the hypothesis that the PO-opt method performs with better robustness in gait phase estimation and walking/standing state classification than the original one, which is beneficial to eliminating jittering during transition gaits. To test our hypothesis, we used a portable hip exoskeleton incorporated with both PO and PO-opt estimation methods and designed trials with typical daily life transition gaits, walking to standing, during a series of multimodal locomotion. The contributions of this study are listed as follows. Firstly, we proposed a robust and low computing power cost PO-opt algorithm to reduce the continuous gait phase estimation error in a real-time application. This is an important contribution to robotic exoskeleton control, since the continuous gait phase is a critical state variable that is directly related to accurate assistive torque profile generation. Secondly, the threshold of the lateral axis extreme difference (LAED) was determined and validated in a series of walking-to-stop transition gaits to eliminate jittering caused by gait phase error and random disturbance from the user. Our work is intended to make inroads toward improved, yet simplistically implemented, gait phase estimation and autonomous exoskeleton control for application in daily life scenarios.

2. Methods

2.1. Portable hip exoskeleton

The robotic hip exoskeleton used to assist the participants' hip joints in the sagittal plane consists of powered joint modules, interface modules (cuffs and frames), and electric modules (control board and battery) as shown in Fig. 1. This study utilized a previously designed portable hip exoskeleton [27], which is lightweight and autonomous. The powered joint module is composed of a servo motor (Maxon EC 90 Flat, Maxon motor Co., Ltd, Switzerland), a customized planetary gear reducer, and a motor driver (ESCON 50/5 module, Maxon motor Co., Ltd, Switzerland) on the left and right sides, providing assistive torque for flexion and extension. The waist and leg straps are designed referring to lower limb orthoses, which is able to accommodate the subject's waist and legs for better force transmission. The overall structure of our device is mainly composed of aluminum alloy, carbon fiber, and plastic, and the total weight is 3.5 kg. Each actuated joint output power reaches up to 200 W and provides a nominal torque of 17.8 Nm and a peak torque of 37.8 Nm.

Two inertial measurement units (Shenzhen Witte Intelligent Technology Co., Ltd, China) (IMUs) were mounted on the front of the thigh straps bilaterally to measure the hip flexion/extension angle and angular velocity. The control architecture of our device consists of sensing, decision, and execution layers. In the sensing layer, the microprocessor reads the IMU data through the serial port. Our PO-opt algorithm is implemented in the decision layer, which estimates the gait phase in real time and thus generates the assistive torque. In the execution layer, the commanded torque, consisting of the
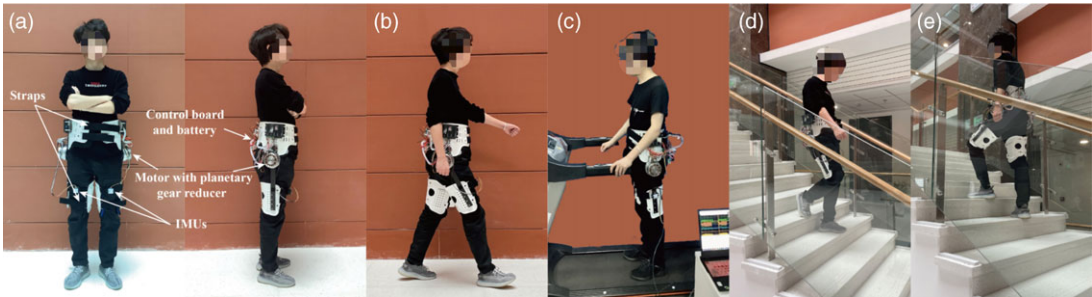
Figure 1. *(a) Front and left view of the portable hip exoskeleton. (b), (c), (d), and (e) Multimodal locomotion trials of free walking, treadmill walking, stair descent, and stair ascent.*

desired assistive torque, and friction and inertia torques, is sent to the motor driver. In the motor driver, a closed-loop PID torque controller is applied to output the correct torque to the subject. The control board realizes wireless data transmission with the host computer through Bluetooth to realize real-time monitoring of the control system status.

2.2. PO optimization

The original phase variables were calculated from the angle and angular velocity of the thigh, which were measured by the IMU mounted on the thigh, with a sampling frequency of 200 Hz. PO is a simple, robust, and effective method to estimate the gait phase of cyclic walking, running, and jumping motion because it only depends on the current human–machine motion state [24, 26]. The gait phase φ of PO can be calculated according to the following equation:

$$\varphi = \text{atan2}(\dot{\theta}, \theta) \tag{1}$$

where θ and $\dot{\theta}$ represent the current joint angle and angular velocity, respectively.

PO transforms gait data (such as hip joint flexion and extension angle) from time domain to phase domain. The phase portrait formed by angle and angular velocity is an ellipse during each gait cycle. By making the orbit in the phase plane more circular, the linearity of gait phase in the time domain can be improved [28, 29]. The adaptive phase shift and scale strategies are as follows:

$$\begin{cases} \hat{\theta}(t) = s(t) \times (\theta(t) + \alpha(t)) \\ \dot{\hat{\theta}}(t) = -(\dot{\theta}(t) + \beta(t)) \end{cases} \tag{2}$$

where $s(t)$ is the scale factor, and $\alpha(t)$ and $\beta(t)$ are the shift factors for hip angle and angular velocity, respectively. The normalization factors, $s(t)$, $\alpha(t)$, and $\beta(t)$, that help to focus the phase portrait around the origin are defined as:

$$s(t) = \left| \frac{\dot{\theta}_{\max}(t) - \dot{\theta}_{\min}(t)}{\theta_{\max}(t) - \theta_{\min}(t)} \right| \tag{3}$$

$$\alpha(t) = -\left(\frac{\theta_{\max}(t) + \theta_{\min}(t)}{2} \right) \tag{4}$$

$$\beta(t) = -\left(\frac{\dot{\theta}_{\max}(t) - \dot{\theta}_{\min}(t)}{2} \right) \tag{5}$$

where $\theta_{\max}(t)$, $\theta_{\min}(t)$, $\dot{\theta}_{\max}(t)$, and $\dot{\theta}_{\min}(t)$ are the max/min joint angles, max/min joint angular velocities, respectively, within one gait cycle. During each gait cycle, these parameters can be obtained through the following equations:

$$\theta_{\min}(t) = \min\left\{\theta(\hat{t}) \,\middle|\, \hat{t} \in \left[t_{\theta_{\max}}, t\right)\right\} \tag{6}$$

$$\dot{\theta}_{\min}(t) = \min\left\{\dot{\theta}(\hat{t}) \,\middle|\, \hat{t} \in \left[t_{\dot{\theta}_{\max}}, t\right)\right\} \tag{7}$$

$$\theta_{\max}(t) = \max\left\{\theta(\hat{t}) \,\middle|\, \hat{t} \in \left[t_{\theta_{\min}}, t\right)\right\} \tag{8}$$

$$\dot{\theta}_{\max}(t) = \max\left\{\dot{\theta}(\hat{t}) \,\middle|\, \hat{t} \in \left[t_{\dot{\theta}_{\min}}, t\right)\right\} \tag{9}$$

where $t_{\theta_{\max}}$, $t_{\theta_{\min}}$, $t_{\dot{\theta}_{\max}}$, and $t_{\dot{\theta}_{\min}}$ correspond to the timings of the max/min angle and angular velocity, respectively, in the previous gait cycle.

Each step generates a clockwise phase portrait in the phase plane. There are visible differences between the phase portrait of walking and standing gaits. We proposed the definition of the LAED that classifies the different gaits:

$$x_{\text{LAED}} = \hat{\theta}_{\max}(t) - \hat{\theta}_{\min}(t) \tag{10}$$

where x_{LAED} stands for the value of LAED, $\hat{\theta}_{\max}(t)$ and $\hat{\theta}_{\min}(t)$ are max/min shifted and scaled angles in one gait cycle, respectively. According to Eq. (5), x_{LAED} is the maximum value on the lateral axis of the phase portrait for the previous gait cycle. $\hat{\theta}_{\max}(t)$ and $\hat{\theta}_{\min}(t)$ are obtained by:

$$\hat{\theta}_{\min}(t) = \min\left\{\hat{\theta}(\hat{t}) \,\middle|\, \hat{t} \in \left[t_{\hat{\theta}_{\max}}, t\right)\right\} \tag{11}$$

$$\hat{\theta}_{\max}(t) = \max\left\{\hat{\theta}(\hat{t}) \,\middle|\, \hat{t} \in \left[t_{\hat{\theta}_{\min}}, t\right)\right\} \tag{12}$$

where the max/min time values $t_{\hat{\theta}_{\max}}$ and $t_{\hat{\theta}_{\min}}$ correspond to the timings of the max/min shifted and scaled angles of the previous gait phase.

We proposed two hypotheses as follows: (1) x_{LAED} is different in the state of walking and standing so that threshold x_{thr} can be used to determine the current locomotion state; and (2) x_{thr} in various walking scenarios is different, which may also be affected by assistive torque, walking speed and other factors. Comparing x_{LAED} with a certain LAED threshold x_{thr}, the locomotion state can be classified;

$$\text{state} = \begin{cases} \text{walking}, & x_{\text{LAED}} \geq x_{\text{thr}} \\ \text{standing}, & x_{\text{LAED}} < x_{\text{thr}} \end{cases} \tag{13}$$

With the help of adaptive phase shift and scale, the difference of gait portrait in phase plane is much clearer between the state of walking and standing. The threshold x_{thr} is used to judge the states. When it is greater than the threshold, it is considered to be walking; otherwise, it is considered to be standing, so as to set the commanded torque to be zero to eliminate unnecessary jittering.

When the subject wears a hip exoskeleton and starts to walk from standing state, the gait trajectory in phase plane will start from the origin and draw irregular ellipses. However, when the subject stops and stands from walking, the minor shake or some other excess mis movements of the subject will be regarded as the user's subjective actions by the exoskeleton. The corresponding angle and angular velocity signals will be introduced into PO model to generate assistive torque, which is applied to the subject to enlarge uncertain mis movement, finally causing the oscillation to diverge. This phenomenon is shown as the continuous jittering during walking-to-stop transition gaits. In fact, the actual phase orbit of standing state always turns to irregular movements near the origin rather than the ellipses of walking state.

2.3. Experimental protocol

The experimental protocol consisted of three sessions: (1) treadmill walking with various speeds, (2) level-ground free walking with various assistive torques, and (3) multimodal scenarios walking-to-stop tests. The goal of the experimental protocol was to study the influence of various walking speeds and

Table I. *Subject information.*

Subject	Gender	Body weight	Height	Age
1	Male	53.5 kg	1.62 m	23 years
2	Male	72.0 kg	1.75 m	24 years
3	Male	56.0 kg	1.73 m	26 years
4	Male	72.0 kg	1.70 m	35 years
5	Male	72.0 kg	1.82 m	22 years
Mean ± std	N/A	64.9 ± 8.7 kg	1.72 ± 0.07 m	26 ± 5 years
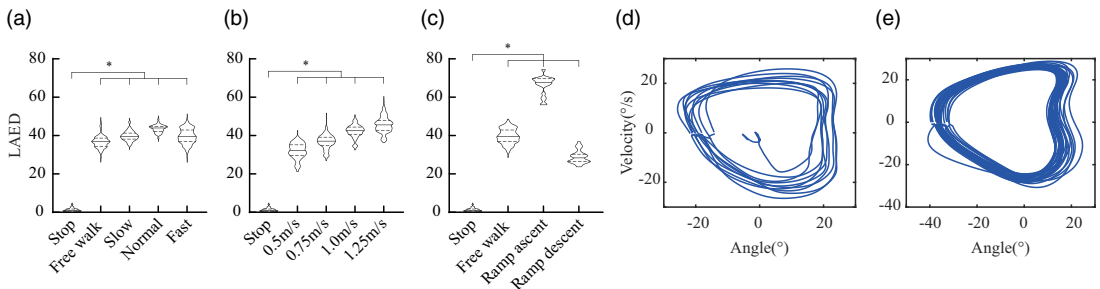
Figure 2. *LAED values and gait phases calculated from the database in different conditions. (a) Level-ground walking with a slow, normal, and fast self-selected speeds. (b) Treadmill walking with constant speeds (0.5 m/s, 0.75 m/s, 1.0 m/s, and 1.25 m/s). (c) Multimodal walking (free walking, ramp ascent, and ramp descent). (d) and (e) The gait phases of free walking and treadmill walking with the PO-opt model.*

assistive torques for PO-opt-based jittering elimination and find the optimal LAED threshold that classifies walking and standing states to eliminate jittering in multimodal scenarios. As shown in Table I, five subjects participated in all sessions. Informed consents were obtained from the subjects. The ethics committee of the College of Biomedical Engineering and Instrument Science of Zhejiang University approved the study (202255).

The assistance profile used in the experiment is determined by a sine function:

$$\tau = k \sin(\varphi) \tag{14}$$

where φ is the estimated gait phase that used to calculate the torque. The amplitude of torque is determined by coefficient k and adjusted in the experiment.

In session 1, assisted by the exoskeleton, the subjects were asked to walk on the treadmill at a constant speed for more than 10 steps and then stop. The speed of the treadmill was set at 3, 4, and 5 km/h, respectively. In each speed case, the subjects were asked to repeat walk and stop at least 20 times wearing the exoskeleton with PO-opt model and PO model, respectively. The assistive torque amplitude was 10 Nm. The divergent jittering of the exoskeleton was observed and recorded manually.

In session 2, the subjects walked on level ground at a self-selected speed with exoskeleton assistance. They walked for more than 10 steps with the assistive torque amplitude of 10 Nm and 5 Nm, respectively, and stopped. Each case repeated for at least 20 times wearing the exoskeleton with PO-opt model and PO model, respectively. The divergent jittering of the exoskeleton was observed and recorded manually.

In session 3, the subjects were asked to walk upstairs and downstairs with the assistive torque amplitude of 10 Nm. According to the results from the database simulation (Fig. 2), in each case, x_{thr} was set at 5.0, 10.0, 15.0, and 20.0, respectively, in the PO-opt model. The subjects stopped after at least 10 steps and repeated at least 10 times for both upstairs and downstairs wearing the exoskeleton with PO-opt model. The divergent jittering of the exoskeleton was observed and recorded manually.

2.4. Data processing

In this study, database from ref. [30] and experimental data from multimodal walking trials were simulated and validated, respectively.

For the offline simulation part, in order to select an appropriate LAED threshold, x_{thr}, we utilized MATLAB (MathWorks, Natick, Massachusetts, USA) to analyze the database [30]. Gait data were derived from the walking trials of different locomotion modes, such as treadmill walking, level-ground walking, and ramp ascent/descent (inclination angle is 16.2°). The speeds for treadmill trials were 0.5 m/s, 0.75 m/s, 1.0 m/s, and 1.25 m/s, and in level-ground walking the average pelvis velocities over all subjects were 0.88 ± 0.19 m/s, 1.17 ± 0.21 m/s and 1.45 ± 0.27 m/s for slow, normal, and fast self-selected speeds, respectively. In each case, the gait data were collected from more than 5 subjects in at least 10 trials, totaling at least 100 gait cycles [30]. PO-opt model was used to calculate x_{LAED} of each gait cycle.

For the online validation part, a microprocessor (STM32F103RET6, STMicroelectronics, Geneva, Switzerland) was used to sample sensor data and then transmitted the experiment data to the computer through J-Link (SEGGER Microcontroller Systems LLC, USA) every 2 ms. Aiming at optimizing PO model, we studied the influence of various walking speeds and torques on jittering elimination, counted the success times of each walking trial manually, and determined the interval of x_{thr} that classified walking and standing states clearly. In offline simulation, the LAED threshold value has been preliminarily obtained with various scenarios (treadmill walking, level-ground walking, and ramp ascent/descent), while in online validation experiment, more attention was paid to multimodal (treadmill, free walking, and stair ascent/descent) scenarios which is much closer to daily life to verify whether the LAED threshold is appropriate. The gait data were obtained during multimodal (treadmill, free walking, and stair ascent/descent) walking trials in the aforementioned three sessions. For each condition, at least 10 trials totally 100 gait cycles were taken to calculate the mean and standard deviation of angle and angular velocity. The success rate was defined as the percentage of the gait cycles that the standing state was successfully recognized in the walking-to-stop transition gaits.

3. Results

3.1. Threshold selection

For x_{thr} selection, we utilized the gait data from database [30] to offline simulate x_{LAED} in various scenarios. As shown in Fig. 2, x_{LAED} of standing state fell in the area between 0.21 and 4.13, which was significantly smaller than that of the walking state (from 28.73 to 48.58). For the treadmill walking case, as the walking speed increased from 0.5 m/s to 1.25 m/s with 0.25 m/s increments, the medians of x_{LAED} also increased, which were 32.21, 37.06, 42.61, and 45.54, respectively. x_{LAED} varies in multimodal locomotion such as free walking, ramp ascent/descent, and stair ascent/descent, which mainly results from the difference in the max/min flexion/extension angles of the hip joint during various walking scenarios.

According to the above offline simulation results, x_{thr} was preliminarily selected as 15.0, which was able to classify walking and standing states during treadmill walking, free walking, and ramp ascent/descent. The phase portrait in Fig. 3d illustrates that the phase diagram of the actual walking is not a standard ellipse, but the phase trajectory of each step is always formed clockwise around the origin.

3.2. System performance with transition gaits

To verify the performance of both PO and PO-opt estimators, walking-to-stop transition gaits from treadmill walking trials (3 km/h speed, 10 Nm assistive torque) were studied first. Raw thigh angles and angular velocities measured by the IMUs were processed by a fourth-order Butterworth low-pass filter (5 Hz cutoff). Based on the filtered gaits, we used both PO and PO-opt to estimate gait phases. Figure 3 shows the output gait phases of both estimators in the time domain and phase plane. As expected, the
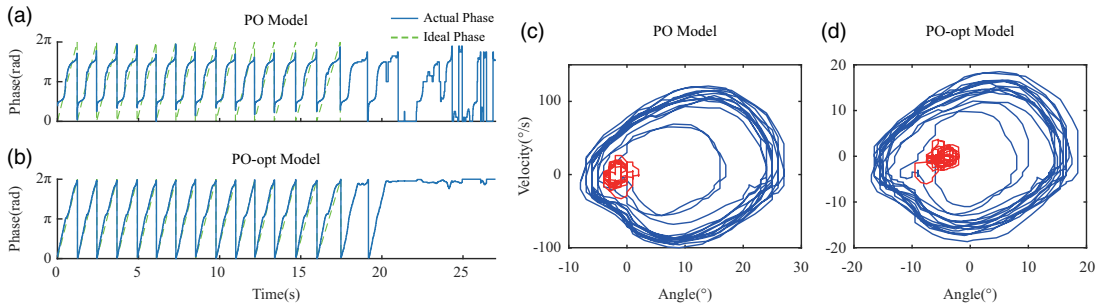
Figure 3. *The gait phase of PO model and PO-opt model from treadmill walking trials (3 km/h speed, 10 Nm assistive torque). (a) and (b) Gait phase in time domain estimated by PO model and PO-opt model. (c) and (d) Gait phase in phase plane estimated by PO model and PO-opt model. Red and blue lines are standing and walking states, respectively.*

phase linearity of the PO-opt model in the time domain was significantly improved. Compared with the ideal case (phase varies uniformly in a gait cycle from 0% to 100%), the normalized phase linearity of PO model and PO-opt model is 0.101 and 0.059, respectively, in which the linearity of PO-opt model has increased by 41.6%.

In this case, when the subject stopped and stood still, the phase of PO model jumps much more (Fig. 3a) than that of PO-opt model (Fig. 3b), making it easier to oscillate and diverge at this time. Figure 3c, d show the gait phase portraits of PO model and PO-opt model in phase plane, with red and blue lines representing standing and walking states, respectively. The phase portrait of PO-opt model is more approximate to an ellipse, and the center of the portrait is closer to the origin. This is because the size and position of the phase portrait are more unified due to adaptive shift and scale, which facilitates the classification of walking and standing states with LAED.

3.3. Walking trials

In sessions 1 and 2, the preliminarily selected x_{thr} from offline simulation was applied to the PO-opt model for online exoskeleton-assisted walking trials. Specifically, hip joint angles, angular velocities, and gait phases result of one treadmill walking trial (3 km/h speed, 10 Nm assistive torque), one free walking trial with low assistive torque (5 Nm), and one free walking trial with high assistive torque (10 Nm) are plotted in Fig. 4a, b, Fig. 4c, d, and Fig. 4e, f, respectively. Results of both PO model (Fig. 4a, c, e) and PO-opt model (Fig. 4b, d, f) are shown for comparison. In all three trials, the hip joint angles converged to a certain value close to zero with PO-opt model during standing states, while the hip joint angles oscillated and diverged with PO model, which indicated that the PO-opt model can better eliminate jittering for transition gaits. Meanwhile, the resulted gait phases of PO-opt model show better linearity. In addition, compared to low assistive with PO model in free walking scenario, the jittering is more violent for high assistive torque.

3.4. Multimodal scenarios locomotion trials

In session 3, stair ascent/descent walking trials were carried out. For each locomotion scenario (treadmill walking, free walking, and stair ascent/descent), the hip joint angle and angular velocity were averaged within one gait cycle and shown in Fig. 5. For treadmill walking, various speeds could somehow affect the hip joint angle profile of the same subject (Fig. 5a). For free walking, different subjects preferred different self-selected walking speeds and performed significantly different amplitudes of angle profiles (Fig. 5b). The angle profiles of stair ascent and descent vary significantly, which indicates different lower limb postures during stair ascent and descent.
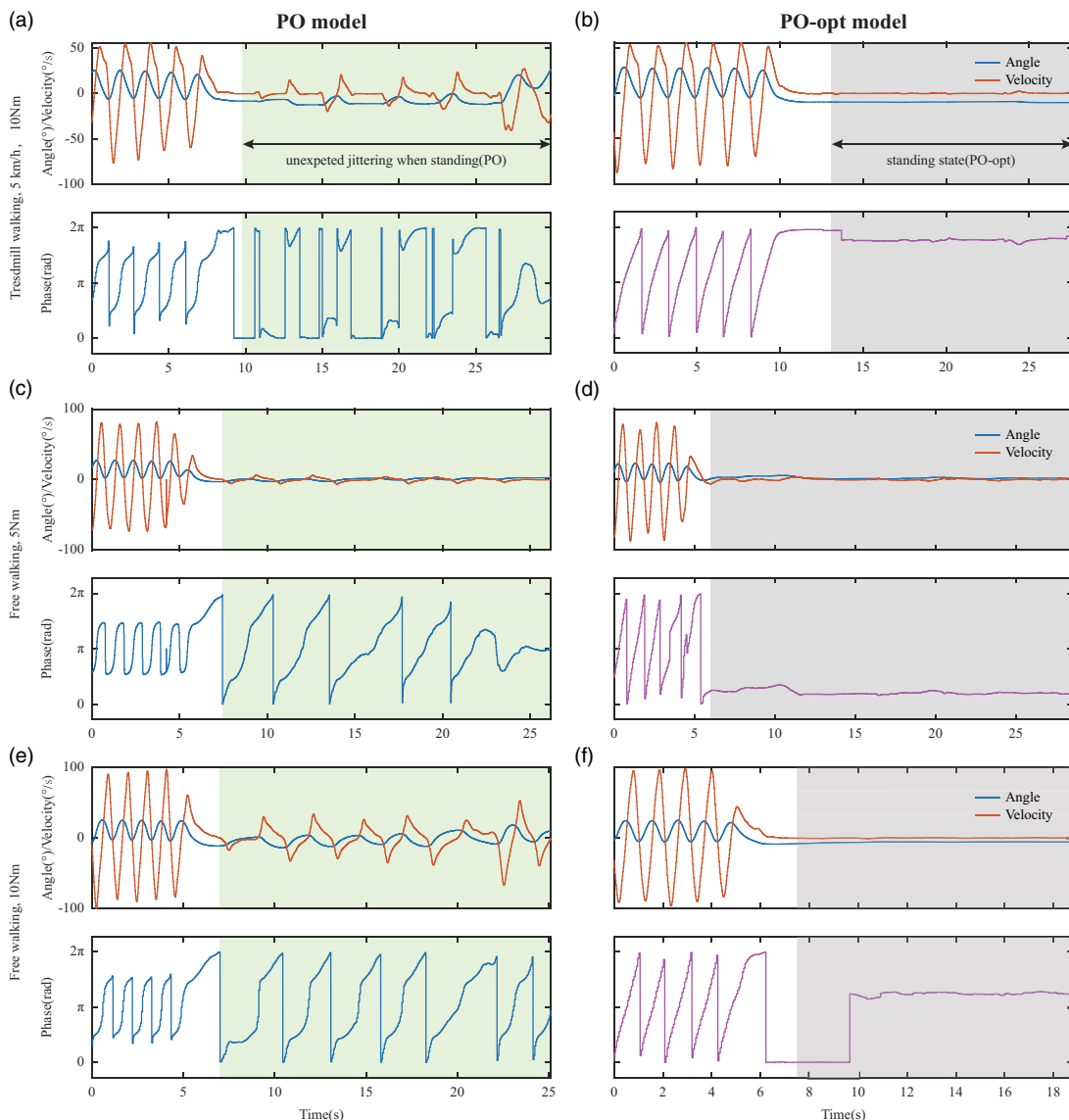
Figure 4. *Comparison of jittering in multimodal locomotion trials. The left and right columns, respec-*
tively, represent the results of PO model and PO-opt model. The gray shadow represents standing period,
and green shadow represents the unexpected jittering during standing states. (a) and (b) illustrate walk-
ing at 3 km/h on the treadmill with assistive torque amplitude of 10 Nm. (c) and (d) Free walking on
level ground with assistive torque amplitude of 5 Nm. (e) and (f) Free walking on level ground with
assistive torque amplitude of 10 Nm. The upper half of each subfigure shows angle and angular velocity,
which are represented by blue and orange lines, respectively; the lower half of each subfigure shows
gait phase and walking/standing state. The blue and purple lines represent phase with PO model and
PO-opt model, respectively.

For treadmill walking trials, the rate of success to eliminate jittering was calculated at each speed,
which was defined as the proportion of the number of tests that successfully eliminated jittering to the
number of all tests (at least 20 trials for each case). As shown in Fig. 5d, compared to the PO model, the
rate of success of 3, 4, and 5 km/h treadmill walking with the PO-opt model increased from 29%, 21%,
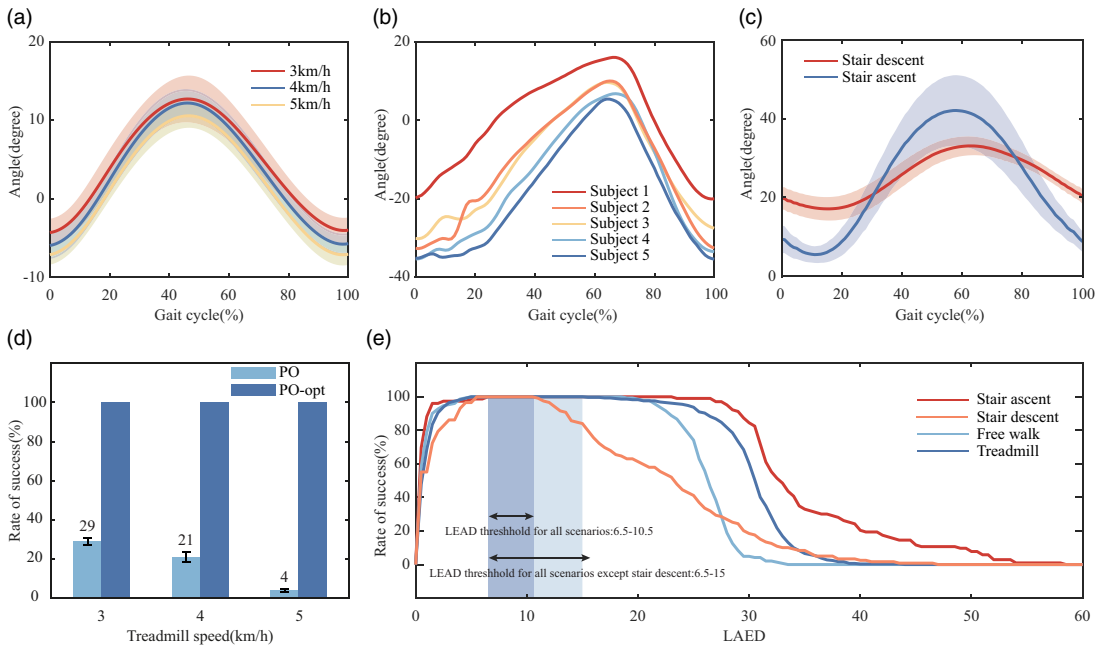
Figure 5. *Multimodal locomotion trials results. (a) Averaged hip angles of five subjects in a gait cycle (treadmill walking with 3, 4, and 5 km/h speeds). The mean angle is shown in a line with a standard deviation range shown in a shadow. (b) Hip angles of five subjects in a gait cycle (free walking). (c) Averaged hip angles of five subjects in a gait cycle (stair ascent/descent). The mean angle is shown in a line with a standard deviation range shown in a shadow. (d) Rate of success of jittering elimination at different treadmill speeds (3, 4, and 5 km/h) of PO model without optimization and PO-opt model, respectively. (e) Threshold of LAED for multimodal locomotion. Dark blue and light blue shadows represent the best range of LAED threshold values for all scenarios and all that except stair descent, respectively.*

and 4% to 100%, 100%, and 100%, respectively. With the PO-opt model, the jittering in transition gaits can be well eliminated.

For stair ascent/descent trials, since the hip joint angle profiles vary obviously, the phase portraits may also vary. For the offline simulation part based on our stair ascent/descent trials data, we calculated the rate of success when x_{thr} was set from 1 to 20 with 1 increment. For the online validation part, we manually recorded the jittering when x_{thr} was set at 5.0, 10.0, 15.0, and 20.0. At least 10 trials were carried out for each x_{thr} during both stair ascent and descent. According to the results in Fig. 5e, either large or small x_{thr} will reduce the rate of success for jittering elimination. A suitable range that classifies walking and standing states may be from 6.5 to 10.5. Based on the above results, the applicable threshold interval in multimodal scenarios falls from 6.5 to 10.5, and the applicable threshold interval in multimodal scenarios except stair descent is from 6.5 to 15.0.

4. Discussion

The primary goal of this study was to validate a practical gait phase estimation and hip exoskeleton control scheme that robustly recognizes the transition gaits and eliminates divergent jittering during daily life walking across multimodal scenarios. The estimated gait phase with original PO during standing state is disordered (Fig. 3a), which should be a constant value. This phenomenon mainly results from the large angular velocity and small angle (close to zero) caused by unexpected human–exoskeleton interaction. As the gait phase determines the assistive torque profile, a disordered gait phase during standing

state is prone to cause a disordered assistive torque profile, leading to divergent jittering. Meanwhile, applying an accurate gait phase estimator is the foundation of reducing the user's metabolic cost which has been considered a "gold standard" outcome measure in the field of exoskeleton [16]. Researches have shown that assistance timing (which is directly related to the gait phase) is a critical index for assistive torque profile parameterization. Based on previous studies [31–34], Kang et al. pointed out that approximately 10% change in the assistance onset or peak timing can correlate up to 2.5% (on average) in metabolic expenditure difference [16]. Consequently, we "shift" and "scale" the phase portrait to filter the gait phase for better linearity and "slice" the phase portrait to classify and detect walking and standing states correctly during transition gaits. The results indicate that the PO-opt estimator is beneficial to improving the gait phase estimation and eliminating the jittering in transition gaits.

We firstly simulated the LAED results during multimodal scenarios based on gait data from Young's group [30]. From the simulation results shown in Fig. 2, the LAED of the stop state (transition gait from walking-to-stop) is significantly lower than those of various-speed free walking, treadmill walking, and ramp ascent/descent as well. Specifically, the LAED medians of various-speed free walking and treadmill walking mainly locate between 32.21 and 45.55, while the LAED median of ramp ascent is significantly higher (67.71) and that of ramp descent is lower (28.37). This comes from the variety of gaits during various scenarios. Applying the LAED results to the PO-opt estimator, our hip exoskeleton was verified to eliminate divergent jittering during walking-to-stop transition gaits as shown in Figs. 4 and 5. The red and blue curves in the phase portrait, which correspond to standing and walking states, respectively, illustrate differences of both states directly. Without PO optimization, the jittering is prone to diverge during stop state as shown in Fig. 4a, c, e (green area). This can mainly be attributed to disordered assistive torque by exoskeleton, which caused larger angular velocity during stop state.

The rate of success results in Fig. 5d indicate that the faster the treadmill speed was set, the lower rate of success with PO model would be. One possible reason is that a more intense walking–standing transition (stop suddenly from a high walking speed) can lead to more posture adjustments of the user, which is easier to trigger jittering of the exoskeleton. However, the rate of success of 3, 4, and 5 km/h treadmill walking with the PO-opt model can reach up to 100%, indicating that the method is effective at different walking speeds. Interestingly, during stair descent trials, the jittering elimination rate was quite low when the LAED was set at 15.0, which was an applicable threshold for free walking, treadmill walking, and stair ascent. We simulated the jittering elimination rate with variable LAED values based on the data from our stair descent trials. The simulation results meet the experimental results well and demonstrate that during stair descent scenario, the LAED range (6.5–10.5 for 100% rate of success) reduces significantly for jittering elimination, which is far lower than that of the other three scenarios (6.5–15.0 for 100% rate of success). This can mainly be attributed to a smaller range of motion of hip flexion/extension during stair descent as shown in Fig. 5c. Consequently, a more rigorous LAED range should be determined when the hip exoskeleton-assisted walking scenarios contain stair descent.

5. Conclusion

In this article, we systematically evaluated gait phase estimation performance of two PO-based estimators, PO and PO-opt, during the hip exoskeleton-assisted walking-to-stop transition gaits in multimodal scenarios. The key findings of the study showed a significant increase in jittering elimination rate by application of the PO-opt model. To our best knowledge, this is the first research that studies gait phase estimation of daily life transition gaits for hip exoskeleton control, which is a step toward filling the gap in the application of the portable exoskeleton from laboratory to the real world. Furthermore, the proposed PO-opt estimator could be used by prostheses and other types of exoskeletons. Future work should more specifically study how assistive torque could be generated to control a portable hip exoskeleton for daily life walking assistance with variable transition gaits, based on the current progress of both user preference [13] and human-in-the-loop optimization [4, 22].

References

[1] C. Yang, L. Yu, L. Xu, Z. Yan, D. Hu, S. Zhang and W. Yang, "Current developments of robotic hip exoskeleton toward sensing, decision, and actuation: A review," *Wearable Technol.* **3**, E15 (2022). doi: 10.1017/wtc.2022.11.

[2] Z. Li, Y. Yuan, L. Luo, W. Su, K. Zhao, C. Xu, J. Huang and M. Pi, "Hybrid brain/muscle signals powered wearable walking exoskeleton enhancing motor ability in climbing stairs activity," *IEEE Trans. Med. Robot. Bionics* **1**(4), 218–227 (2019). doi: 10.1109/tmrb.2019.2949865.

[3] Q. Wei, Z. Li, K. Zhao, Y. Kang and C.-Y. Su, "Synergy-based control of assistive lower-limb exoskeletons by skill transfer," *IEEE/ASME Trans. Mechatron.* **25**(2), 705–715 (2020). doi: 10.1109/tmech.2019.2961567.

[4] J. Kim, G. Lee, R. Heimgartner, D. Arumukhom Revi, N. Karavas, D. Nathanson, I. Galiana, A. Eckert-Erdheim, P. Murphy, D. Perry, N. Menard, D. K. Choe, P. Malcolm and C. J. Walsh, "Reducing the metabolic rate of walking and running with a versatile, portable exosuit," *Science* **365**(6454), 668–672 (2019). doi: 10.1126/science.aav7536.

[5] G. Lv, H. Zhu and R. D. Gregg, "On the design and control of highly backdrivable lower-limb exoskeletons: A discussion of past and ongoing work," *IEEE Control Syst.* **38**(6), 88–113 (2018). doi: 10.1109/MCS.2018.2866605.

[6] G. S. Sawicki, O. N. Beck, I. Kang and A. J. Young, "The exoskeleton expansion: Improving walking and running economy," *J. Neuroeng. Rehabil.* **17**(1), 25 (2020). doi: 10.1186/s12984-020-00663-9.

[7] V. L. Chiu, M. Raitor and S. H. Collins, "Design of a hip exoskeleton with actuation in frontal and sagittal planes," *IEEE Trans. Med. Robot. Bionics* **3**(3), 773–782 (2021). doi: 10.1109/tmrb.2021.3088521.

[8] G. M. Bryan, P. W. Franks, S. C. Klein, R. J. Peuchen and S. H. Collins, "A hip-knee-ankle exoskeleton emulator for studying gait assistance," *Int. J. Robot. Res.* **40**(4-5), 722–746 (2020). doi: 10.1177/0278364920961452.

[9] D. F. N. Gordon, C. McGreavy, A. Christou and S. Vijayakumar, "Human-in-the-loop optimization of exoskeleton assistance via online simulation of metabolic cost," *IEEE Trans. Robot.* **38**(3), 1–20 (2022). doi: 10.1109/tro.2021.3133137.

[10] M. K. Ishmael, D. Archangeli and T. Lenzi, "Powered hip exoskeleton improves walking economy in individuals with above-knee amputation," *Nat. Med.* **27**(10), 1783–1788 (2021). doi: 10.1038/s41591-021-01515-2.

[11] H. Han, W. Wang, F. Zhang, X. Li, J. Chen, J. Han and J. Zhang, "Selection of Muscle-Activity-Based Cost Function in Human-in-the-Loop Optimization of Multi-Gait Ankle Exoskeleton Assistance," *IEEE Trans. Neural Syst. Rehabil. Eng.* **29**, 944–952 (2021). doi: 10.1109/TNSRE.2021.3082198.

[12] W. Wang, J. Chen, Y. Ji, W. Jin, J. Liu and J. Zhang, "Evaluation of lower leg muscle activities during human walking assisted by an ankle exoskeleton," *IEEE Trans. Ind. Inform.* **16**(11), 7168–7176 (2020). doi: 10.1109/tii.2020.2974232.

[13] K. A. Ingraham, C. D. Remy and E. J. Rouse, "The role of user preference in the customized control of robotic exoskeletons," *Sci. Robot.* **7**(64), eabj3487 (2022). doi: 10.1126/scirobotics.abj3487.

[14] R. L. Medrano, G. C. Thomas and E. J. Rouse, "Can humans perceive the metabolic benefit provided by augmentative exoskeletons?" *J. Neuroeng. Rehabil.* **19**(1), 26 (2022). doi: 10.1186/s12984-022-01002-w.

[15] G. Li, Z. Li, C.-Y. Su and T. Xu, "Active human-following control of an exoskeleton robot With body weight support," *IEEE Trans. Cybern.* 1–13 (2023). doi: 10.1109/TCYB.2023.3253181.

[16] I. Kang, P. Kunapuli and A. J. Young, "Real-time neural network-based gait phase estimation using a robotic hip exoskeleton," *IEEE Trans. Med. Robot. Bionics* **2**(1), 28–37 (2020). doi: 10.1109/tmrb.2019.2961749.

[17] T. Yan, A. Parri, V. R. Garate, M. Cempini, R. Ronsse and N. Vitiello, "An oscillator-based smooth real-time estimate of gait phase for wearable robotics," *Auton. Robot.* **41**(3), 759–774 (2016). doi: 10.1007/s10514-016-9566-0.

[18] E. Zheng, S. Manca, T. Yan, A. Parri, N. Vitiello and Q. Wang, "Gait phase estimation based on noncontact capacitive sensing and adaptive oscillators," *IEEE Trans. Biomed. Eng.* **64**(10), 2419–2430 (2017). doi: 10.1109/TBME.2017.2672720.

[19] K. Seo, K. Kim, Y. J. Park, J-K. Cho, J. Lee, B. Choi, B. Lim, Y. Lee and Y. Shim, "Adaptive Oscillator-Based Control for Active Lower-Limb Exoskeleton and its Metabolic Impact," **In:** *2018 IEEE International Conference on Robotics and Automation (ICRA)* (2018) pp. 6752–678. doi: 10.1109/ICRA.2018.8460841.

[20] J. Buchli, L. Righetti and A. J. Ijspeert, "Frequency analysis with coupled nonlinear oscillators," *Physica D* **237**(13), 1705–1718 (2008). doi: 10.1016/j.physd.2008.01.014.

[21] T. Lenzi, M. C. Carrozza and S. K. Agrawal, "Powered hip exoskeletons can reduce the user's hip and ankle muscle activations during walking," *IEEE Trans. Neural Syst. Rehabil. Eng.* **21**(6), 938–948 (2013). doi: 10.1109/TNSRE.2013.2248749.

[22] J. Zhang, P. Fiers, K. A. Witte, R. W. Jackson and S. H. Collins, "Human-in-the-loop optimization of exoskeleton assistance during walking," *Science* **356**(6344), 1280–1283 (2017).

[23] I. Kang, D. D. Molinaro, S. Duggal, Y. Chen, P. Kunapuli and A. J. Young, "Real-time gait phase estimation for robotic hip exoskeleton control during multimodal locomotion," *IEEE Robot. Autom. Lett.* **6**(2), 3491–3497 (2021). doi: 10.1109/lra.2021.3062562.

[24] T. G. Sugar, A. Bates, M. Holgate, J. Kerestes, M. Mignolet, P. New, R. K. Ramachandran, S. Redkar and C. Wheeler, "Limit cycles to enhance human performance based on phase oscillators," *J. Mech. Robot.* **7**(1), (2015). doi: 10.1115/1.4029336.

[25] J. De la Fuente, S. C. Subramanian, T. G. Sugar and S. Redkar, "A robust phase oscillator design for wearable robotic systems," *Robot. Auton. Syst.* **128**, 103514 (2020). doi: 10.1016/j.robot.2020.103514.

[26] J. De la Fuente, T. G. Sugar and S. Redkar, "Nonlinear, phase-based oscillator to generate and assist periodic motions," *J. Mech. Robot.* **9**(2), (2017). doi: 10.1115/1.4036023.

[27] W. Yang, L. Xu, L. Yu, Y. Chen and C. Yang, "Hybrid oscillator-based no-delay hip exoskeleton control for free walking assistance," *Ind. Robot* **48**(6), 906–914 (2021).

[28] W. Hong, N. A. Kumar and P. Hur, "A phase-shifting based human gait phase estimation for powered transfemoral prostheses," *IEEE Robot. Autom. Lett.* **6**(3), 5113–5120 (2021). doi: 10.1109/lra.2021.3068907.

[29] D. Quintero, D. J. Lambert, D. J. Villarreal and R. D. Gregg, "Real-time continuous gait phase and speed estimation from a single sensor," *Control Technol. Appl.* **2017**, 847–852 (2017). doi: 10.1109/CCTA.2017.8062565.

[30] J. Camargo, A. Ramanathan, W. Flanagan and A. Young, "A comprehensive, open-source dataset of lower limb biomechanics in multiple conditions of stairs, ramps, and level-ground ambulation and transitions," *J. Biomech.* **119**(108), 110320 (2021). doi: 10.1016/j.jbiomech.2021.110320.

[31] Y. Ding, F. A. Panizzolo, C. Siviy, P. Malcolm, I. Galiana, K. G. Holt and C. J. Walsh, "Effect of timing of hip extension assistance during loaded walking with a soft exosuit," *J. Neuroeng. Rehabil.* **13**(1), 87 (2016). doi: 10.1186/s12984-016-0196-8.

[32] S. Galle, P. Malcolm, S. H. Collins and D. De Clercq, "Reducing the metabolic cost of walking with an ankle exoskeleton: Interaction between actuation timing and power," *J. Neuroeng. Rehabil.* **14**(1), 35 (2017). doi: 10.1186/s12984-017-0235-0.

[33] P. Malcolm, W. Derave, S. Galle and D. De Clercq, "A simple exoskeleton that assists plantarflexion can reduce the metabolic cost of human walking," *PLoS One* **8**(2), e56137 (2013). doi: 10.1371/journal.pone.0056137.

[34] A. J. Young, J. Foss, H. Gannon and D. P. Ferris, "Influence of power delivery timing on the energetics and biomechanics of humans wearing a hip exoskeleton," *Front. Bioeng. Biotechnol.* **5**, 4 (2017). doi: 10.3389/fbioe.2017.00004.